10. T. Gorecki, "The relations between the shear modulus, the bulk modulus, and Young's modulus for polycrystalline metallic elements," Mater. Sci. Engng., 43, No. 3 (1980).
11. S. I. Meshkov, "Quasiresonance method of determining the relaxation spectrum parameters," Mechanisms of Relaxation Phenomena in Solids [in Russian], Nauka, Moscow (1972).

AXIALLY SYMMETRICAL COLLAPSE OF SPALLED LAYERS IN A CYLINDRICAL STEEL SHELL

A. G. Ivanov, V. N. Sofronov,
and E. S. Tyun'kin

UDC 539.415

There are several papers (see for example [1, 2] and bibliography there) on the spalling-free collapse of cylindrical shells as far as complete condensation. However, conditions frequently arise in explosion experiments that lead to spalling. Here we present results on the deformation and spalling in cylindrical steel shells on explosive loading, and we also give a theoretical description.

The loading intensity was such that the energy received by the shell was insufficient for complete collapse. We used shells made of St. 3 steel of outside diameter 47.6 mm, wall thickness 8.8 mm, and length 150 mm.

The loading was produced by a sliding detonation wave DW excited in a charge of TG 50/50 explosive placed directly on the outer surface. The DW was excited from one of the ends simultaneously around the circle by means of an explosive disk initiated at the center.

Figure 1 shows the shells after use. Table 1 gives the charge thicknesses Δ, the dimensions of the cross sections after loading (diameter and wall thickness), the thickness of the spalled layer, the shell strains ε, and the thickness of the spalled layer at the time of formation. The last was determined on the assumption that the layer arises by reflection of the first shock wave from the free boundary, when the displacement of the shell wall is slight (this assumption does not conflict with the calculations). The shell dimensions (Table 1) were obtained by averaging not less than 10 measurements.

The sections shown in Fig. 1 illustrate the effects of explosive layer thickness on the spalling damage as well as features of the spalled layer collapse. In all cases where the explosive thickness was less than the shell wall thickness, spalling occurred; spalling-free collapse occurred only in experiment 1 (Fig. 1a), where the explosive layer thickness was 10 mm.

In experiments 2 and 3 (Fig. 1b and c, explosive layer thicknesses respectively of 7.5 and 5 mm), the spalled layer collapsed stably without disintegration and became thicker by factors of 1.5 and 2.3 respectively, the strains being 35 and 38.5%.

On reducing the explosive thickness to 3 and 2 mm (Fig. 1d and e), the spalled layer broke up into fragments of size about 3 × 5 mm because of shear deformation and consequent loss of stable collapse. Finally, at a thickness of 1 mm (Fig. 1f) one gets the initial stage of spalling: A principal crack is generated and perturbations occur in the spalled layer. The strain in the remaining shell is also very much dependent on the charge thickness. When that thickness varies by a factor 10 (from 1 to 10 mm), ε varies by a factor 24 (from 0.84 to 20.4%), and the relationship is linear for charge thicknesses in the range 1-5 mm, but then there is a sharp increase accompanied by the occurrence of bending perturbations, which had the largest amplitude ($\Delta r/r \sim 3\%$) in experiment 2, where the deformation was quite large ($\varepsilon \sim 13.7\%$) and the thickness of the remaining shell was small. The number of perturbations in the shell was about 10, and the perturbations were not strictly periodic.

Moscow. Translated from Zhurnal Prikladnoi Mekhaniki i Tekhnicheskoi Fiziki, No. 3, pp. 125-127, May-June, 1984. Original article submitted April 15, 1983.

 0021-8944/84/2503-0452$08.50

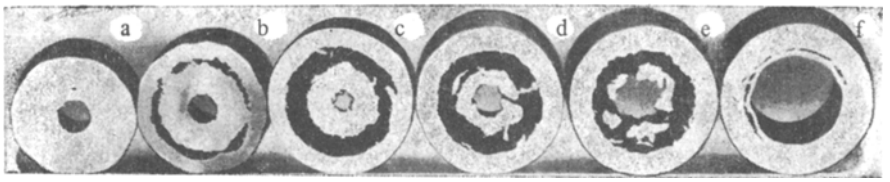

Fig. 1

TABLE 1

Experiment number, figure	Charge thickness Δ, mm	Dimensions of shell section after experiment, mm	Dimensions of spalled layer, mm	Shell strain ϵ, %	Spalled layer thickness at time of formation, mm
1 Fig. 1a	10	37,8×13,6	—	20,4	—
2 Fig. 1b	7,5	41×4,9	28×9...10	13,7	6,6
3 Fig. 1c	5	45,7×5,8	23×8...8,5	4,2	3,7
4 Fig. 1d	3	46,3×6,6	24×3...5	2,53	2,5
5 Fig. 1e	2	46,7×7,2	21×3...5	1,68	1,8
6 Fig. 1f	1	47,2×7,5	31×1,5...2	0,84	1,6

However, these features of the collapse naturally cannot be reflected in one-dimensional calculations. It is thus clear that the ratio of the charge and shell thicknesses determines whether one gets spalling-free collapse or spalling.

The deformation of a cylindrical shell produced by an external explosion has been considered numerically. We incorporated the radial motion about the symmetry axis. As a sliding explosion is not one-dimensional, the calculations were based on instantaneous detonation for the entire layer. The expansion of the detonation products was described by a cubic equation of state with $\rho_0 = 1.51$ g/cm^3 and $D = 7.8$ km/sec.

The motion and deformation were calculated on the basis of effects such as compressibility, elasticity, plasticity, and failure.

The model was that of a Maxwell viscoelastic body [3]. Interpolation formulas were used to approximate the dependence of the internal energy and tangential-stress relaxation time on the parameters of the medium [4, 5]. A Neumann difference scheme (cross) with artificial viscosity was used in solving the differential equations.

The spalling was described as in [6]; the spalling criterion was equality between the stored elastic energy in the stretched zone and the energy E_λ required to produce a new surface:

$$2\pi \int_{r_i}^{r_c} E_{el}\, \rho r dr = 2\pi r_{sp} E_\lambda,$$

where r_i and r_c are the radii of the boundaries of the stretching zone, and r_{sp} is the radius at which the spalling occurs. We took E_λ as 0.09 J/mm^2. The elastic energy has two components: that from the volume change and that from the shape change:

$$E_{el} = (1/2)\left[c_0^2 - (4/3)\, b_0^2\right](\delta - 1)^2 l_0(\delta) + 2b_0^2 l_1(\delta)\, D.$$

Here we have used the symbols of [5].

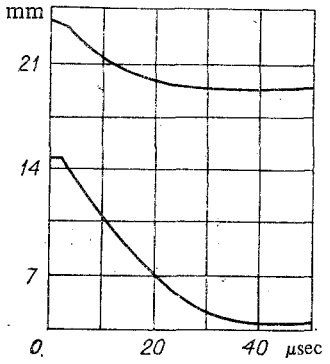

Fig. 2

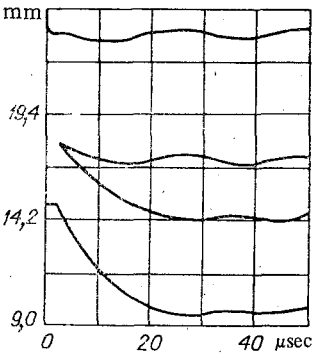

Fig. 3

Two problems were solved. With given dimensions for the steel shell (diameter 47.6 × 8.8 mm), we varied the explosive thickness. In the first calculation, Δ = 10 mm, and in the second Δ = 5 mm.

During the calculation we corrected the value of parameter q appearing in the expression for the relaxation time and characterizing the relation between the shear and elastic stresses. The calculations were performed with $q = 0.6 \times 10^4$ instead of $q = 2.6 \times 10^4$ [5], which increases the contribution from the elastic stresses. This change in q was made because in [5] the particular type of steel was not given. Therefore, to elucidate the effects of the type of steel, we made a comparison experiment with Armco iron with 10-mm charges. It was found that a difference from experiment 1 with St. 3, where the shell did not collapse, was that there was complete condensation with the Armco iron. This effect was incorporated by varying q in the preliminary calculations.

Figure 2 shows the r—t diagram for shell collapse on loading by a charge of thickness 10 mm. The outer boundary of the shell begins to move at t = 0, and the inner one at about 1.6 μsec. The motion of the boundaries involves a delay, and a halt occurs at 35 μsec. The final halt radius at the internal boundary was 4.9 mm, which was close to the experimental value. The initial speeds of the boundaries were 190 and 520 m/sec (outer and inner respectively), which were also close to the values derived from the initial explosive pulse.

The collapse of the shell was accompanied by a temperature rise, which was about 35°K in the shock wave and about 700°K at the maximum.

The kinetic energy attained its maximum at 4 μsec after the start, and after 35 μsec it had been converted to thermal energy, which was practically equal to the total energy.

Figure 3 shows the r—t diagram for loading by a charge of thickness 5 mm; at 2.6 μsec a spalling layer of thickness about 3 mm is formed at a radius of 18 mm, which converges towards the center and thickens to about 4.7 mm. The remaining wall is almost undisplaced, but it oscillates about the initial position. The temperature rise in the shock wave is also about 35°K, but the final temperature is somewhat lower (about 500°K) than in the previous experiment because of the smaller initial velocity.

Therefore, the model provides a qualitative description of the collapse of a cylindrical shell, which is also quantitative for certain parameters. There are certain discrepancies from the experiment (on the spalling thickness and the absence of deformation in the outer boundary), which evidently could be eliminated by appropriate choice of the computation parameters.

LITERATURE CITED

1. N. I. Matyushkin and Yu. A. Trishin, "Some effects arising in the explosive compression of a viscous cylindrical shell," Zh. Prikl. Mekh. Tekh. Fiz., No. 3 (1978).
2. A. G. Ivanov, V. N. Mineev, and E. S. Tyun'kin, "Pulsed collapse of a steel cylindrical shell," Izv. Akad. Nauk SSSR, MTT, No. 2 (1982).
3. S. K. Godunov, Elements of the Mechanics of Continuous Media [in Russian], Nauka, Moscow (1978).
4. S. K. Godunov, N. S. Kozin, and E. I. Romenskii, "The equation of state for the elastic energy in a metal with a nonspherical deformation tensor," Zh. Prikl. Mekh. Tekh. Fiz., No. 2 (1974).

5. S. K. Godunov, V. V. Denisenko, et al., "Use of a viscoelastic relaxation model in calculating uniaxial homogeneous strains and refining interpolation formulas for Maxwellian viscosity," Zh. Prikl. Mekh. Tekh. Fiz., No. 5 (1979).
6. A. G. Ivanov, "Spalling in the quasiacoustic approximation," Fiz. Goreniya Vzryva, No. 3 (1975).

CALCULATION AND EXPERIMENTS ON THE DEFORMATION OF EXPLOSION-CHAMBER SHELLS

A. I. Abakumov, V. V. Egunov, A. G. Ivanov,
A. A. Uchaev, V. I. Tsypkin, and A. T. Shitov

UDC 620.178.7

It has been observed that there is a cyclic increase in the strain amplitude with the passage of time in experiments on the pulsed loading of explosion chambers [1, 2], which is due to interaction between some bending modes of the chamber called the critical with membrane forms of vibration, which results in an unstable state, with cyclic energy transfer from the membrane forms to the bending ones. The bending forms are excited by various structural components (tubes, supporting plates for instruments, welded joints, and so on), and also by imperfections represented by deviations in the geometrical and mechanical characteristics.

Here we compare theoretical results with experimental ones to show that the cyclic strain growth can be described by means of a shell theory of Timoshenko type incorporating the rotating inertia and the transverse shear.

1. Experimental Scheme and Results. We examined the deformation of a closed spherical shell made of steel 35 of internal radius 153 mm and thickness 13.5 mm filled with air under normal conditions when a charge was exploded within it.

Figure 1 shows the system and the main dimensions. The shell 1 was sealed by the rigidly fixed plug 2 and was suspended from the neck by a sheet of small acoustic rigidity and mass, which eliminated any effect from the supporting system on the dynamic strain. The spherical charge 5 made of TH 50/50 (50% trotyl and 50% hexagen, density 1.65 g/cm^3) was of mass 80 $\pm$ 0.5 g and was placed at the center of the shell and detonated from the center. The possible deviation of the charge center from the geometrical center of the shell was not more than 2 mm. The shell strain $\varepsilon(t)$ was recorded at the equator and pole by strain gauges. In the equator region, the measurement was of the mean axially symmetrical strain performed by two ring wire sensors 3 [3]. In the region of the pole, we recorded the local strain over a baseline of 20 mm with two symmetrically disposed sensors 4. The centers of the sensors deviated from the pole by 10 mm. The recording was performed with S1-18 oscilloscopes. The maximum recording time was 2 msec. The maximum error in determining the strain was 10% and in the time intervals was 5%.

Table 1 gives the results of two identical experiments, where ε_1 and t_1 are correspondingly the strain at the first peak and the time when it was attained reckoned from the start of strain, while ε_{max} and t_{max} are the maximum strain and the time when it was attained. Figure 2, solid lines, shows the observed $\varepsilon(t)$ at the equator and pole obtained by averaging the two experiments.

The results show as follows:

1) The average annular strain in the equatorial region and the local strain around the pole coincide during the first half-cycle; and 2) the maximum value of the mean annular strain in the equatorial region occurs during the first half-cycle (Fig. 2), while the maximum local strain at the pole is attained after several periods, i.e., one gets the transfer phenomenon recorded in [1].

Moscow. Translated from Zhurnal Prikladnoi Mekhaniki i Tekhnicheskoi Fiziki, No. 3, pp. 127-130, May-June, 1984. Original article submitted April 29, 1983.

0021-8944/84/2503-0455$08.50